ABCA7 haplodeficiency disturbs microglial immune responses in the mouse brain

Tomonori Aikawa[a], Yingxue Ren[b], Yu Yamazaki[a], Masaya Tachibana[a,1], Madeleine R. Johnson[a], Casey T. Anderson[a], Yuka A. Martens[a], Marie-Louise Holm[a], Yan W. Asmann[b], Takashi Saito[c,2], Takaomi C. Saido[c], Michael L. Fitzgerald[d], Guojun Bu[a], and Takahisa Kanekiyo[a,3]

[a]Department of Neuroscience, Mayo Clinic, Jacksonville, FL 32224; [b]Department of Health Sciences Research, Mayo Clinic, Jacksonville, FL 32224; [c]Laboratory for Proteolytic Neuroscience, RIKEN Center for Brain Science, 351-0198 Wako, Saitama, Japan; and [d]Lipid Metabolism Unit and Center for Computational and Integrative Biology, Massachusetts General Hospital, Harvard Medical School, Boston, MA 02114

Edited by Bruce S. McEwen, Rockefeller University, New York, NY, and approved October 15, 2019 (received for review May 17, 2019)

Carrying premature termination codons in 1 allele of the *ABCA7* gene is associated with an increased risk for Alzheimer's disease (AD). While the primary function of ABCA7 is to regulate the transport of phospholipids and cholesterol, ABCA7 is also involved in maintaining homeostasis of the immune system. Since inflammatory pathways causatively or consequently participate in AD pathogenesis, we studied the effects of *Abca7* haplodeficiency in mice on brain immune responses under acute and chronic conditions. When acute inflammation was induced through peripheral lipopolysaccharide injection in control or heterozygous *Abca7* knockout mice, partial ABCA7 deficiency diminished proinflammatory responses by impairing CD14 expression in the brain. On breeding to $App^{NL\text{-}G\text{-}F}$ knockin mice, we observed increased amyloid-β (Aβ) accumulation and abnormal endosomal morphology in microglia. Taken together, our results demonstrate that ABCA7 loss of function may contribute to AD pathogenesis by altering proper microglial responses to acute inflammatory challenges and during the development of amyloid pathology, providing insight into disease mechanisms and possible treatment strategies.

ABCA7 | Alzheimer's disease | amyloid-β | CD14 | immune response

While brain accumulation of amyloid-β (Aβ) peptides is a principal event in the pathogenesis of Alzheimer's disease (AD), current evidence increasingly recognizes the predominant contribution of the microglia-mediated immune system to disease development and progression (1, 2). In most neurodegenerative diseases, chronic inflammation causes neuronal damage, which likely occurs through the interactive activation among microglia, astrocytes, and vascular endothelial cells in the brain (3). Nonetheless, acute microglial activation mediates beneficial mechanisms for eliminating Aβ and cell debris in some disease phases during AD progression (2). Interestingly, microglia constitute a major cell type in the brain, expressing susceptible loci for late-onset AD, including *APOE*, *TREM2*, *SORLA*, *CR1*, *CD33*, *MS4A*, and *ABCA7* (4). Therefore, there is an urgent need to dissect how the brain immune system causatively affects the complex pathogenesis of AD.

Among the genetic factors, premature termination in one allele of *ABCA7* caused by nonsense, frameshift, and splice site mutations results in its loss of function, which has clearly been associated with the increased risk for late-onset AD (5–8) as well as early-onset AD (9). *ABCA7* encodes ATP-binding cassette (ABC) transporter A7, sharing 54% sequence homology with ABCA1 (10). As a member of the ABC transporter family, ABCA7 participates in the efflux of cellular cholesterol and phospholipids in various cell types (11–15). Of note, accumulating evidence indicates that ABCA7 plays a critical role not only in mediating lipid metabolism, but also in immune responses (16). ABCA7 deficiency diminishes phagocytic ability in fibroblasts (17) and macrophages (18–20) and impairs cytokine responses in natural-killer T cells (21). While previous reports have demonstrated that *Abca7* deletion aggravates Aβ pathology in several human amyloid precursor protein (APP) transgenic amyloid models (22–24), ABCA7 is likely involved in the phagocytic clearance of Aβ oligomers in mouse brains (25). Therefore, exploring ABCA7 functions in brain immune responses should provide critical clues for understanding the pathogenic pathways in AD.

In this study, using heterozygous *Abca7* knockout mice, we investigated the roles of ABCA7 in acute brain immune responses induced by peripheral lipopolysaccharide (LPS) stimulation. Since AD is a chronic disorder in which Aβ pathology precedes the disease onset by approximately 2 decades (26), we also assessed microglial activation in the presence of amyloid pathology. Here we show that ABCA7 haplodeficiency predominantly diminishes acute microglial activation, while Aβ accumulation and endosomal compartments in microglia are altered in the presence of amyloid pathology. Taken together, our results imply that microglial dysregulation is possibly correlated with

Significance

Alzheimer's disease (AD), characterized by progressive neurodegeneration and brain accumulation of amyloid-β (Aβ) and tau, is the leading cause of dementia in the elderly. While increasing genetic studies have demonstrated that loss-of-function variants in *ABCA7* are associated with AD risk, the mechanisms of their pathogenic contributions are not well understood. Here we show that ABCA7 haplodeficiency compromises microglial responses by impairing CD14 expression on acute lipopolysaccharide stimulation in mouse models. Furthermore, in the presence of amyloid pathology, ABCA7 haplodeficiency leads to excessive microglial Aβ accumulation accompanied by increased endosomal compartments. Our findings suggest that ABCA7 loss of function is involved in the development and progression of AD by causing microglial dysregulation.

Author contributions: T.A., G.B., and T.K. designed research; T.A., Y.R., Y.Y., M.T., M.R.J., C.T.A., Y.A.M., M.-L.H., Y.W.A., G.B., and T.K. performed research; T.S., T.C.S., and M.L.F. contributed new reagents/analytic tools; T.A., Y.R., Y.Y., M.T., M.R.J., C.T.A., Y.A.M., M.-L.H., Y.W.A., T.S., T.C.S., M.L.F., G.B., and T.K. analyzed data; and T.A., Y.R., Y.Y., M.T., M.R.J., C.T.A., Y.A.M., M.-L.H., Y.W.A., T.S., T.C.S., M.L.F., G.B., and T.K. wrote the paper.

The authors declare no competing interest.

This article is a PNAS Direct Submission.

Data deposition: The RNA-seq data have been deposited in Gene Expression Omnibus DataSets, https://www.ncbi.nlm.nih.gov/gds (accession no. GSE139592).

[1]Present address: United Graduate School of Child Development, Osaka University, 565-0871 Suita, Osaka, Japan.

[2]Present address: Department of Neurocognitive Science, Institute of Brain Science, Nagoya City University Graduate School of Medical Science, Aichi 467-8601, Japan.

[3]To whom correspondence may be addressed. Email: kanekiyo.takahisa@mayo.edu.

This article contains supporting information online at www.pnas.org/lookup/suppl/doi:10.1073/pnas.1908529116/-/DCSupplemental.

First published November 5, 2019.

increased AD risk in individuals carrying *ABCA7* loss-of-function variants.

Results

ABCA7 Haplodeficiency Diminishes the Brain Immune Response on Peripheral LPS Stimulation. To investigate the role of ABCA7 in acute immune response in the brain, we injected LPS intraperitoneally (i.p.) into littermate control, *Abca7* heterozygous ($Abca7^{+/-}$), and *Abca7* homozygous ($Abca7^{-/-}$) knockout mice at age 2 to 3 mo (*SI Appendix*, Fig. S1*A*) and measured the mRNA levels of the major proinflammatory cytokines IL-6, TNF-α, and IL-1β in the cortex (Fig. 1 *A–C*) and hippocampus (Fig. 1 *D–F*) by qRT-PCR at 3.5 h after administration. *Il6*, *Tnf*, and *Il1b* mRNA levels were up-regulated in both the cortex and hippocampus on peripheral LPS stimulation, while there were no substantial differences in baseline mRNA levels of these cytokines. We found that ABCA7 deficiency diminished the immune responses; $Abca7^{+/-}$ mice had lower brain mRNA levels of *Il6*, *Tnf*, and *Il1b* after LPS administration compared with control mice, excluding cortical *Tnf*. $Abca7^{-/-}$ mice showed similar trends in *Il6* and *Tnf* mRNA expression levels but not in *Il1b* expression, although the differences did not reach statistical significance. LPS administration did not influence *Abca7* mRNA levels in mouse brains or microglia (*SI Appendix*, Fig. S1 *B–D*). Since ABCA7 haplodeficiency sufficiently influenced the brain immune responses on LPS stimulation, we used $Abca7^{+/-}$ mice rather than $Abca7^{-/-}$ mice in the subsequent experiments.

To assess the time-dependent effect, we also measured the expression levels of *Il6*, *Tnf*, and *Il1b* mRNA in the cortex and hippocampus at 1, 3.5, 7, and 24 h after i.p. LPS injection into control and $Abca7^{+/-}$ mice at age 2 to 3 mo (*SI Appendix*, Fig. S2). Although LPS injection acutely induced the transient increase of *Il6*, *Tnf*, and *Il1b* mRNA levels in the cortex and hippocampus of control mice after administration, the LPS-induced production of proinflammatory cytokines was substantially suppressed in the brains of $Abca7^{+/-}$ mice. These results indicate that ABCA7 critically mediates LPS-induced acute brain immune responses, and that ABCA7 haplodeficiency sufficiently or predominantly suppresses the pathway. We did not observe any considerable influence of LPS stimulation on ionized calcium binding adaptor molecule-1 (Iba-1) or glial fibrillary acidic protein (GFAP) immunoreactivity in either control or $Abca7^{+/-}$ mice at 3.5 h after administration (*SI Appendix*, Fig. S3).

To assess whether ABCA7 is involved in the process of acute microglial activation, we prepared primary cultures of microglia from control and $Abca7^{+/-}$ mice at postnatal days 0 through 3. qRT-PCR analysis showed that baseline mRNA levels of *Il6* and *Il1b* were considerably lower in primary microglia with ABCA7 haplodeficiency than in control microglia. Following LPS injections, measurements of *Il6, Tnf*, and *Il1b* mRNA levels in microglia at different time points showed increased gene expression, with a peak after 3 to 6 h. However, the responses of *Il6* and *Il1b* after LPS stimulation were diminished/decreased in microglia from $Abca7^{+/-}$ mice after 3 h (Fig. 2 *A–C*), consistent with our results from in vivo models. Since the expression levels of proinflammatory cytokines are regulated predominantly by activation of the NF-κB or MAPK/ERK pathway (27), we examined the phosphorylation of NF-κB, p38 MAPK, and ERK1/2 following LPS stimulation of microglia by Western blot analysis (Fig. 2 *D–F*). NF-κB, p38 MAPK, and ERK1/2 were rapidly phosphorylated; however, microglia from $Abca7^{+/-}$ mice showed suppressed activation of NF-κB, but not p38 MAPK and ERK1/2, in response to LPS stimulation compared with control microglia. These results imply that ABCA7 haplodeficiency primarily interrupts the NF-κB pathway during acute microglia activation, thereby compromising proinflammatory cytokine production in mouse brains after LPS stimulation.

Transcriptomic Profiling Identifies the Innate Immune System as the Main Pathway Impacted by ABCA7 Haplodeficiency and Acute Immune Stimulation. Next, cortical transcripts were profiled by RNA-seq analysis in control and $Abca7^{+/-}$ mice with or without peripheral LPS administration at age 2 to 3 mo. Our results demonstrate that 1,093 transcripts were changed on LPS stimulation among the mouse groups. Seven hundred twenty-seven transcripts (66.5%) were commonly altered by LPS stimulation; 277 (25.3%) and 89 transcripts (8.1%) were dominantly changed in control and $Abca7^{+/-}$ mice, respectively (Fig. 3*A*). In addition, the weighted gene coexpression network analysis (WGCNA) identified several module traits associated with 4 mouse groups (Fig. 3 *B* and *C*). The turquoise module was strongly associated ($P = 4.0 \times 10^{-9}$) within the 4 groups, where "immune response" and "innate immune response" pathways were top-ranked

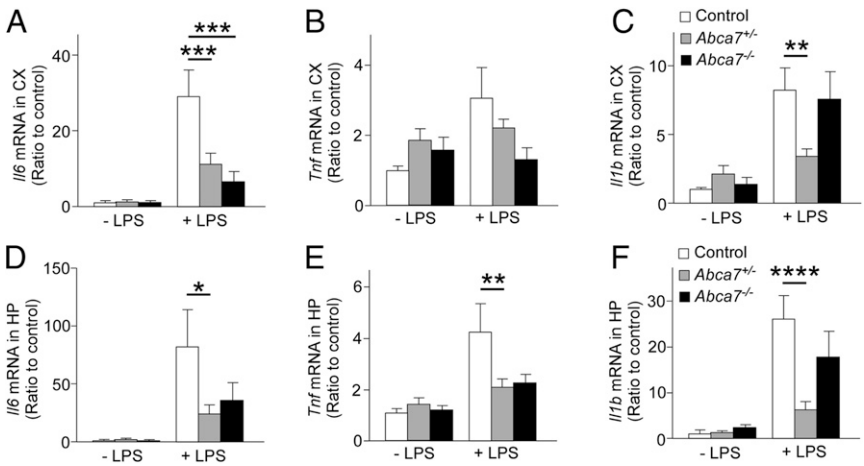

Fig. 1. *Abca7* deficiency suppresses inflammatory cytokine expression in the mouse brain on peripheral LPS administration. mRNA expression levels of inflammatory cytokines were analyzed in the cortex (CX; *A–C*) and hippocampus (HP; *D–F*) of control (white), $Abca7^{+/-}$ (gray), and $Abca7^{-/-}$ (black) mice at 3.5 h after administration with i.p. LPS injection (control, $n = 15$; $Abca7^{+/-}$, $n = 17$; $Abca7^{-/-}$, $n = 9$) or without i.p. LPS injection (control, $n = 16$; $Abca7^{+/-}$, $n = 18$; $Abca7^{-/-}$, $n = 7$). The ΔΔCt values of *Il6* (*A* and *D*), *Tnf* (*B* and *E*), and *Il1b* (*C* and *F*) relative to *Hprt* were measured by qRT-PCR. Relative ratios to control mice without LPS administration are shown as mean ± SEM. $*P < 0.05$; $**P < 0.01$; $***P < 0.001$; $****P < 0.0001$, Tukey–Kramer post hoc analysis of 2-way ANOVA within LPS(−) or LPS(+) groups.

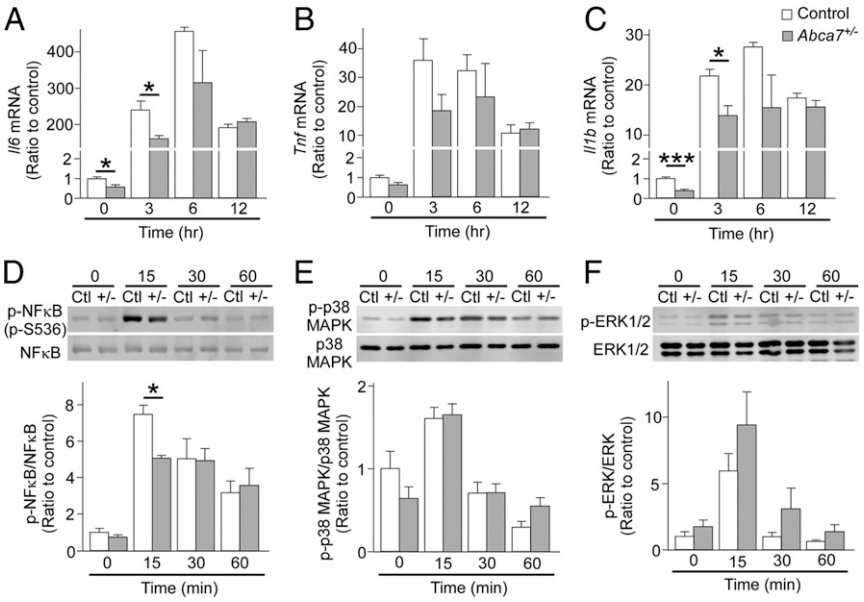

Fig. 2. Delayed immune responses in microglia from heterozygous *Abca7* knockout mice after LPS stimulation. Primary cultures of microglia were prepared from control (white) and *Abca7*$^{+/-}$ (gray) mice. The ΔΔCt values of *Il6* (*A*), *Tnf* (*B*), and *Il1b* (*C*) relative to *Hprt* were measured by qRT-PCR in microglia at 3, 6, and 12 h after culture with LPS (10 ng/mL). Phosphorylation of NF-κB (*D*), p38 MAPK (*E*), and ERK (*F*) was analyzed by Western blotting at 15, 30, and 60 min after culture with LPS. Relative ratios to control microglia without LPS are shown as mean ± SEM (n = 3/each). *P < 0.05; ***P < 0.001, Student t test at each time point.

through Gene Ontology (GO) enrichment analysis (Fig. 3*C*). In addition, gene–gene interaction network analysis in each module (Fig. 3*D* and *SI Appendix*, Table S1) identified *Cd14* as a top-ranked intramodular hub gene in the turquoise module (P = 1.0×10^{-19}). Taken together, these results indicate that ABCA7 haplodeficiency influences brain transcript profiles modified by peripheral LPS administration, and that CD14 or CD14-related pathways may be involved in the altered acute immune response in the brains of *Abca7*$^{+/-}$ mice.

ABCA7 Haplodeficiency Disturbs *Cd14* Expression and Membrane Trafficking on Peripheral LPS Stimulation and When Tested in the Amyloid Background. To validate the RNA-seq results, we measured the mRNA expression of *Cd14* in the cortex (Fig. 3*E*) and hippocampus (Fig. 3*F*) by qRT-PCR at 1, 3.5, 7, and 24 h after i.p. LPS injection into control and *Abca7*$^{+/-}$ mice at age 2 to 3 mo. LPS administration induced an up-regulation of *Cd14* mRNA in the brains of mice in a time-dependent manner, with differing temporal responses between control and *Abca7*$^{+/-}$ mice. *Cd14* mRNA levels were lower in the hippocampus and cortex of *Abca7*$^{+/-}$ mice compared with control mice at 3.5 and 7 h after LPS administration, respectively (Fig. 3 *E* and *F*). We also isolated CD11b-positive microglia from the mouse cortex 7 h after LPS administration and measured *Cd14* mRNA levels (Fig. 3*G*). Although *Cd14* mRNA levels were increased in microglia in both mouse groups after LPS stimulation, the effect was diminished in *Abca7*$^{+/-}$ mice compared with control mice (Fig. 3*G*). Furthermore, quantification of cell surface CD14 levels in CD11b-positive microglia by fluorescence-activated cell sorting (FACS) showed decreased mean fluorescence intensity of CD14 in microglia from *Abca7*$^{+/-}$ mice compared with control mice after peripheral LPS stimulation (Fig. 3*H*). CD14 serves as a coreceptor for Toll-like receptor-4 (TLR-4), and localization of CD14 on the plasma membrane is required for endocytosis of TLR-4 to mediate LPS-induced activation of downstream pathways (28). Thus, our results indicate that ABCA7 haplodeficiency may disturb proper trafficking of CD14 in microglia on LPS stimulation, resulting in compromised induction of *Cd14* mRNA and proinflammatory cytokines in mouse brains.

To investigate how ABCA7 haplodeficiency influences chronic brain inflammation induced by Aβ, we crossed *Abca7*$^{+/-}$ mice with human *APP* knockin mice carrying Swedish, Beyreuther/Iberian, and Arctic mutations (*App*$^{NL\text{-}G\text{-}F/NL\text{-}G\text{-}F}$) (29). We did not observe evident differences in Aβ plaque burden and brain levels of Aβ40 and Aβ42 between control *App*$^{NL\text{-}G\text{-}F/NL\text{-}G\text{-}F}$ mice and *App*$^{NL\text{-}G\text{-}F/NL\text{-}G\text{-}F}$;*Abca7*$^{+/-}$ mice at age 3 mo (*SI Appendix*, Fig. S4). When CD14, a microglial marker (Iba-1), and an early-endosome marker (EEA1) were immunostained in the mouse brains (Fig. 4 *A*–*C*), more CD14 signals were detected in EEA1-positive compartments in Iba-1–positive microglia in the dentate gyrus region of *App*$^{NL\text{-}G\text{-}F/NL\text{-}G\text{-}F}$;*Abca7*$^{+/-}$ mice compared with control *App*$^{NL\text{-}G\text{-}F/NL\text{-}G\text{-}F}$ mice (Fig. 4*C*), although CD14 immunoreactivity in Iba-1–positive microglia was not affected (Fig. 4*B*). In addition, qRT-PCR also demonstrated that ABCA7 haplodeficiency reduced *Cd14* mRNA expression in the hippocampus of *App*$^{NL\text{-}G\text{-}F/NL\text{-}G\text{-}F}$ mice (Fig. 4*D*), consistent with the results from peripheral LPS stimulation. While cell surface CD14 triggers activation of the NF-κB pathway (30), de novo synthesis of CD14 is likely mediated by NF-κB (31). Thus, these results suggest that ABCA7 may be involved in regulating CD14 organelle distribution, thereby modulating *Cd14* mRNA expression in microglia during chronic Aβ stimulation. However, there was a technical limitation in detecting CD14 on the cell surface by immunostaining in mouse brains, and additional studies are needed to confirm our findings. There were no substantial differences in mRNA levels of proinflammatory cytokines and markers for disease-associated microglia (DAM) (32) in the hippocampus between control *App*$^{NL\text{-}G\text{-}F/NL\text{-}G\text{-}F}$ and *App*$^{NL\text{-}G\text{-}F/NL\text{-}G\text{-}F}$;*Abca7*$^{+/-}$ mice (*SI Appendix*, Fig. S5).

ABCA7 Haplodeficiency Leads to Abnormal Microglial Aβ Accumulation and Impaired Endosomal Membrane Trafficking in App$^{NL\text{-}G\text{-}F/NL\text{-}G\text{-}F}$ Mice. To further explore the roles of ABCA7 in microglia in the presence of amyloid pathology, brain sections from control *App*$^{NL\text{-}G\text{-}F/NL\text{-}G\text{-}F}$ and *App*$^{NL\text{-}G\text{-}F/NL\text{-}G\text{-}F}$;*Abca7*$^{+/-}$ mice were stained

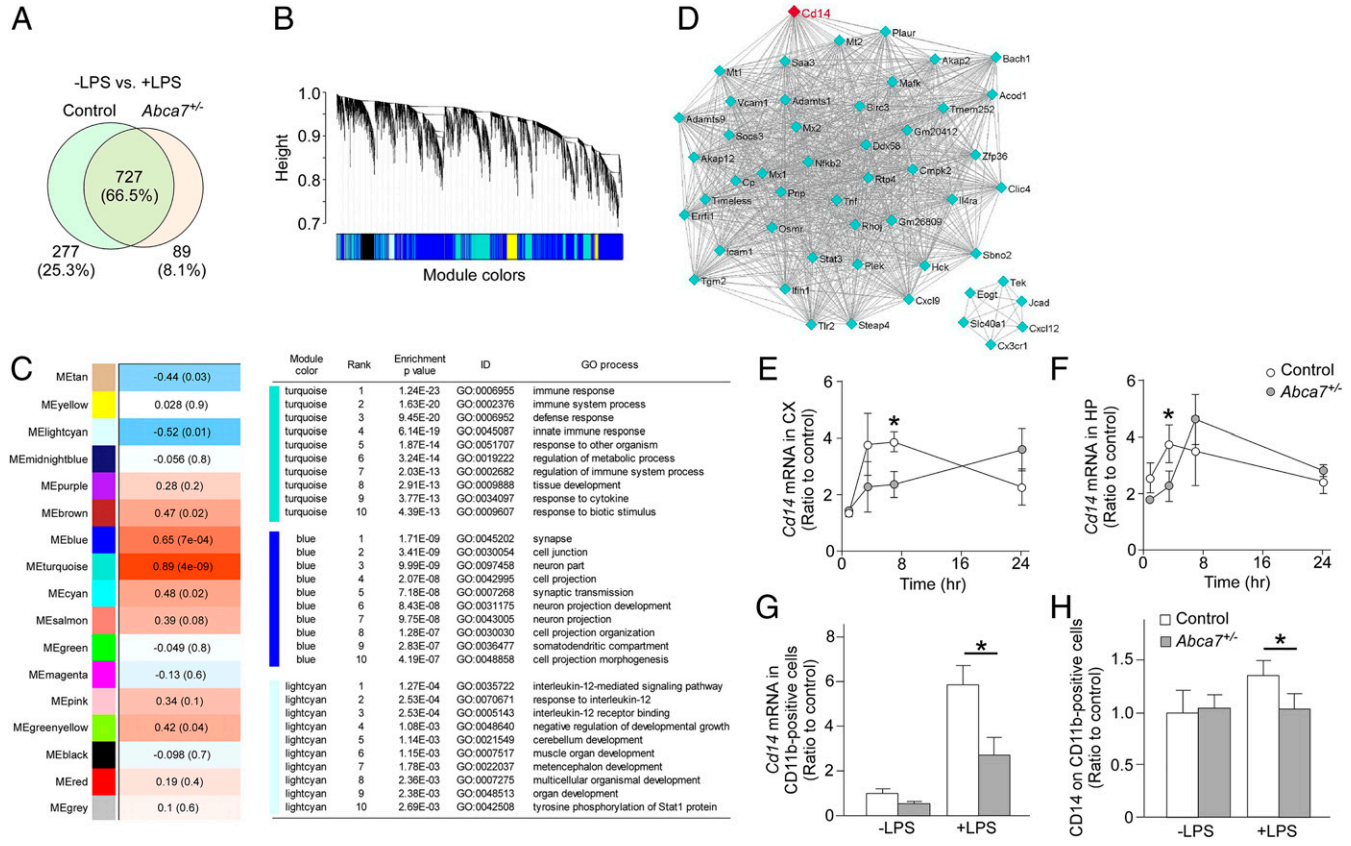

Fig. 3. Altered cortical transcriptome by ABCA7 haplodeficiency and peripheral LPS stimulation. (*A*) Venn diagram of cortical genes markedly changed at 3.5 h after LPS administration in control and *Abca7*$^{+/-}$ mice (n = 6/each) through RNA-seq. (*B*) Clustering dendrogram of genes displayed with gene dissimilarity based on topological overlap through WGCNA among the 4 groups of mice: control with LPS administration, *Abca7*$^{+/-}$ with LPS administration, control with LPS administration, and *Abca7*$^{+/-}$ with LPS administration. Each module is represented by a unique color. (*C*) The module traits were correlated with the 4 groups of mice. The corresponding correlations and *P* values are displayed in each module. Modules showing a significant change ($P \leq 0.01$) were analyzed for pathway enrichment. (*D*) Visualization of the gene–gene interaction within the turquoise module. (*E*–*H*) Expression levels of *Cd14* mRNA were analyzed in the cortex (CX; *E*) and hippocampus (HP; *F*) of control (white) and *Abca7*$^{+/-}$ (gray) mice at 1 h (control, n = 4; *Abca7*$^{+/-}$, n = 4), 3.5 h (control, n = 15; *Abca7*$^{+/-}$, n = 17), 7 h (control, n = 4; *Abca7*$^{+/-}$, n = 4), and 24 h (control, n = 4; *Abca7*$^{+/-}$, n = 4) after i.p. LPS injection. (*G* and *H*) CD11b-positive microglia were isolated from the cortex at 7 h after administration with or without i.p. LPS injection. *Cd14* mRNA (G; control, n = 4; *Abca7*$^{+/-}$, n = 4; control with LPS, n = 9; *Abca7*$^{+/-}$ with LPS, n = 9) and cell surface CD14 (H; control, n = 4; *Abca7*$^{+/-}$, n = 4; control with LPS, n = 9; *Abca7*$^{+/-}$ with LPS, n = 9) levels in the isolated microglia were measured by qRT-PCR and FACS, respectively. For qRT-PCR, the ΔΔCt values of *Cd14* relative to *Hprt* were measured. Relative ratios to control mice without LPS administration are shown as mean ± SEM. *$P < 0.05$, Student *t* test at each time point (*E* and *F*) or Tukey–Kramer post hoc analysis of 2-way ANOVA (*G* and *H*).

for Iba-1, EEA1, and/or Aβ at age 3 mo (Fig. 5*A*). Iba-1 immunoreactivity in the cortex and hippocampus also was not influenced by ABCA7 haplodeficiency (Fig. 5*B*). While Aβ in Iba-1–positive microglia was detected mainly in EEA1-positive compartments in control *App*$^{NL\text{-}G\text{-}F/NL\text{-}G\text{-}F}$ mice, we found that more Aβ accumulated in microglia without colocalizing with EEA1 in *App*$^{NL\text{-}G\text{-}F/NL\text{-}G\text{-}F}$;*Abca7*$^{+/-}$ mice. When Aβ immunoreactivity in Iba-1–positive microglia was quantified, Aβ accumulation in microglia was enhanced in the cortex and hippocampus (CA1 and dentate gyrus) of *App*$^{NL\text{-}G\text{-}F/NL\text{-}G\text{-}F}$;*Abca7*$^{+/-}$ mice compared with control *App*$^{NL\text{-}G\text{-}F/NL\text{-}G\text{-}F}$ mice (Fig. 5*C*), although the localization of Aβ in EEA1-positive compartments in microglia was not affected (Fig. 5*D*).

Next, to investigate how partial ABCA7 deficiency influences cellular organelles in microglia, the late-endosome marker Rab7 and the lysosome marker LAMP1 were also stained in the mouse brains in addition to EEA1 and Iba-1. Measurement of their immunoreactivity in Iba-1–positive microglia revealed more EEA1-positive (Fig. 5*E*) and Rab7-positive (Fig. 5*F*) compartments in Iba-1–positive microglia in the cortex or hippocampus of *App*$^{NL\text{-}G\text{-}F/NL\text{-}G\text{-}F}$;*Abca7*$^{+/-}$ mice compared with control *App*$^{NL\text{-}G\text{-}F/NL\text{-}G\text{-}F}$ mice. However, LAMP1-positive lysosomes in microglia were not affected by ABCA7 haplodeficiency (Fig. 5*G*).

In addition, we also investigated the cellular internalization of FAM-Aβ42 in primary microglia from control and *Abca7*$^{+/-}$ mice, along with its colocalization with EEAI, Rab7, and LAMP1. We found greater EEA1 immunoreactivity in microglia from *Abca7*$^{+/-}$ mice compared with control mice. Although we found no difference in internalized FAM-Aβ42 levels, Aβ in EEA1-positive compartments was increased in microglia from *Abca7*$^{+/-}$ mice (*SI Appendix*, Fig. S6). Taken together, our results indicate that proper endosomal-lysosomal trafficking may be disturbed by ABCA7 haplodeficiency in microglia, resulting in abnormal accumulation of Aβ in microglia.

Discussion

In this study, we demonstrated that ABCA7 contributes to the acute microglial activation on peripheral LPS stimulation by modulating CD14 expression. Consistently, we also found reduced *Cd14* mRNA levels in the hippocampus of *App*$^{NL\text{-}G\text{-}F/NL\text{-}G\text{-}F}$;*Abca7*$^{+/-}$ mice accompanied by greater CD14 accumulation in early endosomes in microglia compared with control *App*$^{NL\text{-}G\text{-}F/NL\text{-}G\text{-}F}$ mice. Although ABCA7 haplodeficiency did not influence the expression of proinflammatory cytokines and DAM markers during

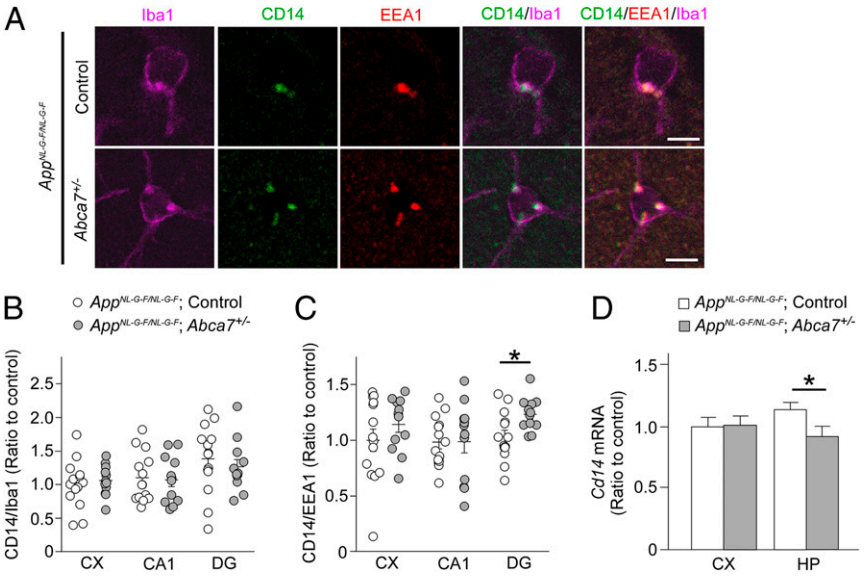

Fig. 4. Influence of ABCA7 haplodeficiency on CD14 in $App^{NL\text{-}G\text{-}F/NL\text{-}G\text{-}F}$ mice. (*A*) Brain sections from $App^{NL\text{-}G\text{-}F/NL\text{-}G\text{-}F}$;control ($n$ = 14) and $App^{NL\text{-}G\text{-}F/NL\text{-}G\text{-}F}$;$Abca7^{+/-}$ mice (n = 12) were immunostained for Iba-1, CD14, and EEA1 at age 3 mo. Representative images from the dentate gyrus region are shown. (Scale bars: 10 μm.) (*B*–*D*) Localization of CD14-positive (*B*) and EEA1-positive (*C*) compartments in Iba-1–positive cells was quantified in the cortex (CX), CA1, and dentate gyrus (DG) of the mice using ImageJ. (*D*) The ΔΔCt values of *Cd14* relative to *Hprt* were measured by qRT-PCR in the cortex and hippocampus (HP). Relative ratios to $App^{NL\text{-}G\text{-}F/NL\text{-}G\text{-}F}$;control mice are shown as mean ± SEM, $*P < 0.05$, Student t test.

brain inflammation related to amyloid pathology, increased or enlarged endosomal compartments in microglia, but not in lysosomes, were detected in $App^{NL\text{-}G\text{-}F/NL\text{-}G\text{-}F}$;$Abca7^{+/-}$ mice along with Aβ accumulation. Furthermore, RNA-seq analysis in control and heterozygous *Abca7* knockout mouse brains followed by WGCNA identified plasma membrane organization and endomembrane system organization as the top-ranked enrichment pathways among modules markedly affected by ABCA7 haplodeficiency (*SI Appendix*, Fig. S7). Thus, ABCA7 loss of function is predicted to interrupt homeostasis of cellular membrane organization, which alters microglial responses during acute and chronic brain inflammation.

Since lipids are the main components of cellular membranes, altered lipid metabolism likely impacts specific stages of the secretory and endosomal pathways (33). While phospholipid asymmetries in the endomembrane system trigger exocytic/endocytic vesicle budding (33), phosphoinositides also contribute to vesicular transport by regulating vesicular budding, membrane fusion, and cytoskeleton dynamics (34, 35). Given that brain phospholipid profiles are altered in $Abca7^{-/-}$ mice (22), it is possible that ABCA7 dysfunction disturbs proper vesicle trafficking by modulating the lipid composition in cellular organelles. Importantly, defects in vesicle trafficking are hallmarks of neurodegeneration, which causatively or consequently contribute to pathogenesis (36). Indeed, endosomal/lysosomal abnormalities are often detected before clinically detectable Aβ deposition in AD (37, 38).

In immune cells, vesicle trafficking plays a critical role in regulating inflammatory responses (39). Interestingly, the pathway in which TLRs mediate responses to their ligands varies depending on cellular localization and trafficking. For example, LPS interacts with TLR-4 and CD14 at the plasma membrane to activate the NF-κB pathway, and their subsequent trafficking into endosomes triggers activation of the interferon regulatory transcription factor 3 (IRF3) pathway (30). While we found that ABCA7 haplodeficiency diminishes activation of the NF-κB pathway in microglia when stimulated with LPS, this could be due to the irregular cell surface distribution and trafficking of CD14. Consistently, ABCA7 deficiency has been shown to compromise lipid raft trafficking on the plasma membrane of antigen-presenting cells, resulting in reduced cell surface CD1d distribution by increasing its accumulation in endosomes (21). Inflammation closely correlates with pathogenic cascades of cognitive impairment and neurodegenerative diseases, including AD (40). While excess activation of the immune system causes harmful neuroinflammation during disease progression, maintenance of the inflammatory environment also plays a neuroprotective role depending on aging, disease stage, and immune mediators (41). In addition, age-related dysregulation of immune responses, termed immunosenescence, not only impacts resistance to infections, but also promotes the development of chronic low-grade inflammation during aging (41). Thus, ABCA7 loss of function possibly may be involved in the immunosenescence processes during aging and AD, although further studies are needed.

Microglia is a dominant brain cell type for cellular uptake and proteostasis of Aβ (42). Interestingly, we found that ABCA7 haplodeficiency increased the accumulation of Aβ in microglia. Since cellular Aβ clearance is likely disturbed in microglia (25) and macrophages (23) from $Abca7^{-/-}$ mice, ABCA7 dysfunction may accelerate Aβ phagocytosis in microglia aberrantly beyond its capacity for degradative elimination or interrupt Aβ trafficking into lysosomes and subsequent proteolysis. In contrast, CD14 has been shown to serve as a scavenger receptor for the fibrillary form of Aβ; a CD14 deficit exacerbates amyloid pathology by suppressing microglial uptake of Aβ (43, 44). Thus, our results indicate that ABCA7 possibly mediates Aβ phagocytosis by microglia independently of CD14.

Furthermore, since endocytosis of APP is likely facilitated in ABCA7-deficient microglia, resulting in aggravated APP processing in endosomes (24), the altered Aβ accumulation observed in microglia of $App^{NL\text{-}G\text{-}F/NL\text{-}G\text{-}F}$;$Abca7^{+/-}$ mice may also be associated with Aβ production as well as with phagocytosis. Since brain inflammation was not affected by ABCA7 haplodeficiency in $App^{NL\text{-}G\text{-}F/NL\text{-}G\text{-}F}$ mice at age 3 mo, future studies should also refine how ABCA7 loss of function impacts the microglial immune responses against prolonged exposure of Aβ without Arc mutation in the aged mouse model. While tau-mediated inflammation was not a focus of this study, further studies might be necessary to

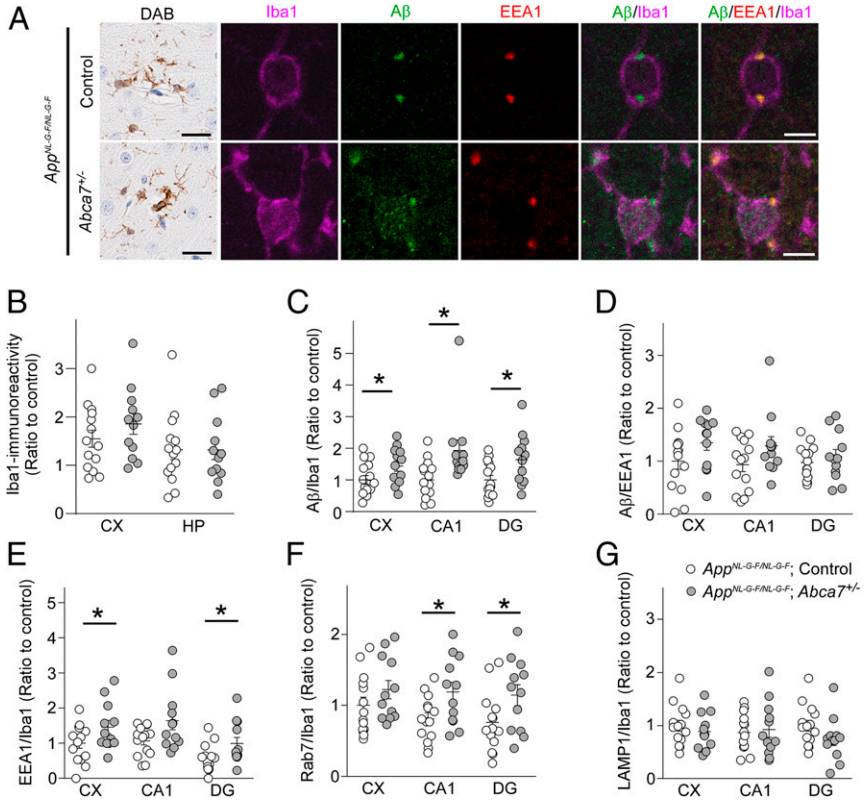

Fig. 5. Microglial Aβ accumulation in $App^{NL\text{-}G\text{-}F/NL\text{-}G\text{-}F}$;$Abca7^{+/-}$ mice. (*A*) Brain sections from $App^{NL\text{-}G\text{-}F/NL\text{-}G\text{-}F}$;control ($n$ = 14) and $App^{NL\text{-}G\text{-}F/NL\text{-}G\text{-}F}$;$Abca7^{+/-}$ mice (n = 12) were immunostained for Iba-1 (DAB; scale bars: 50 μm) and for Iba-1, Aβ, and EEA1 (immunofluorescence; scale bars: 5 μm) at age 3 mo. Representative images from the cortical region for DAB staining and the dentate gyrus (DG) region for immunofluorescence staining are shown. (*B*) DAB immunoreactivity for Iba-1 in the cortex (CX) and hippocampus (HP) were quantified through the Aperio Positive Pixel Count program (Leica Biosystems Imaging). (*C* and *D*) Localization of Aβ in Iba-1–positive cells (*C*) and EEA1-positive compartments in Iba-1–positive cells (*D*) was quantified by ImageJ in the cortex, CA1, and dentate gyrus. (*E*–*G*) Mouse brain sections were also immunostained for Iba-1 and EEA1 (*E*), Rab7 (*F*), and LAMP1 (*G*), and localization in Iba-1–positive cells was quantified. Relative ratios to $App^{NL\text{-}G\text{-}F/NL\text{-}G\text{-}F}$;control mice (CX) are shown as mean ± SEM. *$P < 0.05$, Student t test or the Wilcoxon test.

determine the role of ABCA7 in chronic inflammation in the presence of both Aβ and tau.

Our study reveals that ABCA7 haplodeficiency disrupts the proper immune response during acute microglial activation induced by LPS stimulation, and that microglial Aβ pathology is altered under this chronic condition. These phenotypes produced by ABCA7 dysfunction may be a consequence of membrane disorganization and abnormal membrane trafficking in microglia. Of note, genome-wide association studies in late-onset AD identified the loci clustering predominantly in immune response, lipid metabolism, and endocytosis/intracellular trafficking (4, 45), with ABCA7 involved in all 3 pathways. Therefore, a greater understanding of ABCA7 function should allow us to define molecular mechanisms underlying the cross-talk among immune response, lipid metabolism, and membrane trafficking in AD to develop new therapeutic strategies for severe disease.

Materials and Methods

Animals. All animal procedures were approved by the Mayo Clinic's Institutional Animal Care and Use Committee and were performed in accordance with the National Institutes of Health's *Guide for the Care and Use of Laboratory Animals* (46). *Abca7* knockout mice ($Abca7^{-/-}$) (47) were cross-bred with wild-type C57BL/6 inbred mice. Littermate male $Abca7^{+/+}$, $Abca7^{+/-}$, and $Abca7^{-/-}$ mice were injected i.p. with LPS (5 mg/kg *Escherichia coli* O26:B6; Sigma-Aldrich; L2654) at age 2 to 3 mo. $Abca7^{+/-}$ mice were also bred with $App^{NL\text{-}G\text{-}F/NL\text{-}G\text{-}F}$ mice (29). Both male and female $App^{NL\text{-}G\text{-}F/NL\text{-}G\text{-}F}$;$Abca7^{+/-}$ mice and littermate control $App^{NL\text{-}G\text{-}F/NL\text{-}G\text{-}F}$ mice were used for the analyses at age 3 mo.

Mouse Primary Microglial Culture. Primary cultures of microglia were prepared from wild-type or $Abca7^{+/-}$ mice at postnatal days 0 through 3. Mixed glial cells from the mice were cultured on poly-D-lysine–coated flasks (Sigma-Aldrich; A-003-E) in DMEM (Thermo Fisher Scientific; 11965-084) containing 10% heat-inactivated FBS (Sigma-Aldrich; F2442) and 1% penicillin-streptomycin (Thermo Fisher Scientific; 15140122). The next day, the medium was replaced with medium containing an additional 25 ng/mL of recombinant granulocyte macrophage colony-stimulating factor (Gemini Bio; 300-308P). After 10 to 12 d of culturing, the attached microglia population was harvested by shaking at 200 rpm and used for experiments.

Immunohistochemical Analyses. For 3,3-diaminobenzidine (DAB) staining, paraffin-embedded mouse brain sections were stained with pan-Aβ (clone Aβ 33.1.1; human $Aβ_{1–16}$), Iba-1 (Wako Chemicals USA; 019-19741), and GFAP (BioGenex;, clone GA5) antibodies. Immunoreactivity was measured as percent area of Iba-1–positive pixels after counting the signal intensity in each pixel using the positive pixel count program available with ImageScope software (Aperio Technologies) after scanning using an ImageScope XT image scanner (Aperio Technologies) (22). For immunofluorescence staining, paraffin-embedded mouse brain sections were stained with pan-Aβ (Abcam; ab126649), CD14 (BioLegend; Sa14-2, 123302), Iba-1 (Wako Chemicals USA; 019-19741), LAMP-1 (Abcam; clone H4A3, ab25630), EEA1 (Cell Signaling Technology; 3288), and Rab7 (Cell Signaling Technology; D95F2, 9367) antibodies, followed by incubation with Alexa Fluor 488- or Alexa Fluor 568-conjugated secondary antibodies (Thermo Fisher Scientific). Nuclei were visualized using a mounting medium with DAPI (Vector Laboratories; H-1200). In some experiments, Iba-1 Red Fluorochrome (635)-conjugated antibody (Wako Chemicals USA; 013-26471) was used. Images were obtained using confocal laser-scanning fluorescence microscopy (model LSM 710 inverted; Carl Zeiss). The possibility of cross-reactivity of selected antibodies and

bleed-through of fluorescence emission was ruled out (*SI Appendix*, Fig. S8). The ImageJ JACoP plugin was used for colocalization of signals (48).

Statistics. Statistical significance was determined by Tukey post hoc analysis after 2-way ANOVA or the 2-tailed Student *t* test. Comparisons between 2 datasets with a nonparametric distribution (F test; $P < 0.05$) were assessed using the Wilcoxon test. All statistical analyses were performed with JMP statistical software (SAS Institute) and Microsoft Excel. A P value <0.05 was considered significant.

Data Availability. The RNA-seq data from this study, including the CQN-normalized log2RPKM table, have been deposited into Gene Expression Omnibus (www.ncbi.nlm.nih.gov/geo, accession no. GSE139592) (49).

ACKNOWLEDGMENTS. We thank Dr. Sumiko Abe-Dohmae (Chubu University) for the gift of the ABCA7 antibody. This work was supported by the NIH (Grants R21AG054890, to T.K. and R37AG027924, R01 AG035355, RF1AG056130, and RF1AG051504, to G.B.) and the Cure Alzheimer's Fund (G.B. and T.K.).

1. D. V. Hansen, J. E. Hanson, M. Sheng, Microglia in Alzheimer's disease. *J. Cell Biol.* **217**, 459–472 (2018).
2. H. Sarlus, M. T. Heneka, Microglia in Alzheimer's disease. *J. Clin. Invest.* **127**, 3240–3249 (2017).
3. K. Herrup, Reimagining Alzheimer's disease—An age-based hypothesis. *J. Neurosci.* **30**, 16755–16762 (2010).
4. C. M. Karch, A. M. Goate, Alzheimer's disease risk genes and mechanisms of disease pathogenesis. *Biol. Psychiatry* **77**, 43–51 (2015).
5. M. Allen *et al*., *ABCA7* loss-of-function variants, expression, and neurologic disease risk. *Neurol. Genet.* **3**, e126 (2017).
6. A. C. Naj *et al*., Common variants at MS4A4/MS4A6E, CD2AP, CD33 and EPHA1 are associated with late-onset Alzheimer's disease. *Nat. Genet.* **43**, 436–441 (2011).
7. P. Hollingworth *et al*., Common variants at ABCA7, MS4A6A/MS4A4E, EPHA1, CD33 and CD2AP are associated with Alzheimer's disease. *Nat. Genet.* **43**, 429–435 (2011).
8. C. Reitz *et al*.; Alzheimer Disease Genetics Consortium, Variants in the ATP-binding cassette transporter (ABCA7), apolipoprotein E ∈4, and the risk of late-onset Alzheimer disease in African Americans. *JAMA* **309**, 1483–1492 (2013).
9. A. De Roeck *et al*.; BELNEU Consortium, An intronic VNTR affects splicing of ABCA7 and increases risk of Alzheimer's disease. *Acta Neuropathol.* **135**, 827–837 (2018).
10. W. E. Kaminski *et al*., Identification of a novel human sterol-sensitive ATP-binding cassette transporter (ABCA7). *Biochem. Biophys. Res. Commun.* **273**, 532–538 (2000).
11. S. Abe-Dohmae *et al*., Human ABCA7 supports apolipoprotein-mediated release of cellular cholesterol and phospholipid to generate high-density lipoprotein. *J. Biol. Chem.* **279**, 604–611 (2004).
12. M. L. Fitzgerald *et al*., Naturally occurring mutations in the largest extracellular loops of ABCA1 can disrupt its direct interaction with apolipoprotein A-I. *J. Biol. Chem.* **277**, 33178–33187 (2002).
13. N. Wang, D. L. Silver, P. Costet, A. R. Tall, Specific binding of ApoA-I, enhanced cholesterol efflux, and altered plasma membrane morphology in cells expressing ABC1. *J. Biol. Chem.* **275**, 33053–33058 (2000).
14. N. Wang *et al*., ATP-binding cassette transporter A7 (ABCA7) binds apolipoprotein A-I and mediates cellular phospholipid but not cholesterol efflux. *J. Biol. Chem.* **278**, 42906–42912 (2003).
15. M. Tomioka *et al*., Lysophosphatidylcholine export by human ABCA7. *Biochim. Biophys. Acta Mol. Cell Biol. Lipids* **1862**, 658–665 (2017).
16. T. Aikawa, M. L. Holm, T. Kanekiyo, ABCA7 and pathogenic pathways of Alzheimer's disease. *Brain Sci.* **8**, E27 (2018).
17. N. Iwamoto, S. Abe-Dohmae, R. Sato, S. Yokoyama, ABCA7 expression is regulated by cellular cholesterol through the SREBP2 pathway and associated with phagocytosis. *J. Lipid Res.* **47**, 1915–1927 (2006).
18. A. W. Jehle *et al*., ATP-binding cassette transporter A7 enhances phagocytosis of apoptotic cells and associated ERK signaling in macrophages. *J. Cell Biol.* **174**, 547–556 (2006).
19. N. Tanaka, S. Abe-Dohmae, N. Iwamoto, M. L. Fitzgerald, S. Yokoyama, Helical apolipoproteins of high-density lipoprotein enhance phagocytosis by stabilizing ATP-binding cassette transporter A7. *J. Lipid Res.* **51**, 2591–2599 (2010).
20. N. Tanaka, S. Abe-Dohmae, N. Iwamoto, S. Yokoyama, Roles of ATP-binding cassette transporter A7 in cholesterol homeostasis and host defense system. *J. Atheroscler. Thromb.* **18**, 274–281 (2011).
21. H. N. Nowyhed *et al*., ATP binding cassette transporter ABCA7 regulates NKT cell development and function by controlling CD1d expression and lipid raft content. *Sci. Rep.* **7**, 40273 (2017).
22. N. Sakae *et al*., ABCA7 deficiency accelerates amyloid-β generation and Alzheimer's neuronal pathology. *J. Neurosci.* **36**, 3848–3859 (2016).
23. W. S. Kim *et al*., Deletion of Abca7 increases cerebral amyloid-β accumulation in the J20 mouse model of Alzheimer's disease. *J. Neurosci.* **33**, 4387–4394 (2013).
24. K. Satoh, S. Abe-Dohmae, S. Yokoyama, P. St George-Hyslop, P. E. Fraser, ATP-binding cassette transporter A7 (ABCA7) loss of function alters Alzheimer amyloid processing. *J. Biol. Chem.* **290**, 24152–24165 (2015).
25. Y. Fu, J. H. Hsiao, G. Paxinos, G. M. Halliday, W. S. Kim, ABCA7 mediates phagocytic clearance of amyloid-β in the brain. *J. Alzheimers Dis.* **54**, 569–584 (2016).
26. R. J. Bateman *et al*.; Dominantly Inherited Alzheimer Network, Clinical and biomarker changes in dominantly inherited Alzheimer's disease. *N. Engl. J. Med.* **367**, 795–804 (2012).
27. S. Akira, S. Uematsu, O. Takeuchi, Pathogen recognition and innate immunity. *Cell* **124**, 783–801 (2006).
28. I. Zanoni *et al*., CD14 controls the LPS-induced endocytosis of Toll-like receptor 4. *Cell* **147**, 868–880 (2011).
29. T. Saito *et al*., Single App knock-in mouse models of Alzheimer's disease. *Nat. Neurosci.* **17**, 661–663 (2014).
30. A. F. McGettrick, L. A. O'Neill, Localisation and trafficking of Toll-like receptors: An important mode of regulation. *Curr. Opin. Immunol.* **22**, 20–27 (2010).
31. C. Wagner *et al*., Expression patterns of the lipopolysaccharide receptor CD14 and the FCgamma receptors CD16 and CD64 on polymorphonuclear neutrophils: Data from patients with severe bacterial infections and lipopolysaccharide-exposed cells. *Shock* **19**, 5–12 (2003).
32. H. Keren-Shaul *et al*., A unique microglia type associated with restricting development of Alzheimer's disease. *Cell* **169**, 1276–1290.17 (2017).
33. R. P. Huijbregts, L. Topalof, V. A. Bankaitis, Lipid metabolism and regulation of membrane trafficking. *Traffic* **1**, 195–202 (2000).
34. D. E. Clapham, Calcium signaling. *Cell* **131**, 1047–1058 (2007).
35. J. O. De Craene, D. L. Bertazzi, S. Bär, S. Friant, Phosphoinositides, major actors in membrane trafficking and lipid signaling pathways. *Int. J. Mol. Sci.* **18**, E634 (2017).
36. F. R. Kiral, F. E. Kohrs, E. J. Jin, P. R. Hiesinger, Rab GTPases and membrane trafficking in neurodegeneration. *Curr. Biol.* **28**, R471–R486 (2018).
37. A. M. Cataldo *et al*., Endocytic pathway abnormalities precede amyloid beta deposition in sporadic Alzheimer's disease and Down syndrome: Differential effects of APOE genotype and presenilin mutations. *Am. J. Pathol.* **157**, 277–286 (2000).
38. R. A. Nixon, P. M. Mathews, A. M. Cataldo, The neuronal endosomal-lysosomal system in Alzheimer's disease. *J. Alzheimers Dis.* **3**, 97–107 (2001).
39. A. Prashar, L. Schnettger, E. M. Bernard, M. G. Gutierrez, Rab GTPases in immunity and inflammation. *Front. Cell. Infect. Microbiol.* **7**, 435 (2017).
40. R. L. Ownby, Neuroinflammation and cognitive aging. *Curr. Psychiatry Rep.* **12**, 39–45 (2010).
41. E. Costantini, C. D'Angelo, M. Reale, The role of immunosenescence in neurodegenerative diseases. *Mediators Inflamm.* **2018**, 6039171 (2018).
42. K. I. Mosher, T. Wyss-Coray, Microglial dysfunction in brain aging and Alzheimer's disease. *Biochem. Pharmacol.* **88**, 594–604 (2014).
43. Y. Liu *et al*., LPS receptor (CD14): A receptor for phagocytosis of Alzheimer's amyloid peptide. *Brain* **128**, 1778–1789 (2005).
44. E. G. Reed-Geaghan, J. C. Savage, A. G. Hise, G. E. Landreth, CD14 and Toll-like receptors 2 and 4 are required for fibrillar Aβ-stimulated microglial activation. *J. Neurosci.* **29**, 11982–11992 (2009).
45. G. Tosto, C. Reitz, Genome-wide association studies in Alzheimer's disease: A review. *Curr. Neurol. Neurosci. Rep.* **13**, 381 (2013).
46. National Research Council, *Guide for the Care and Use of Laboratory Animals* (National Academies Press, Washington, DC, ed. 8, 2011).
47. W. S. Kim *et al*., Abca7 null mice retain normal macrophage phosphatidylcholine and cholesterol efflux activity despite alterations in adipose mass and serum cholesterol levels. *J. Biol. Chem.* **280**, 3989–3995 (2005).
48. S. Bolte, F. P. Cordelières, A guided tour into subcellular colocalization analysis in light microscopy. *J. Microsc.* **224**, 213–232 (2006).
49. T. Aikawa *et al*., ABCA7 haplodeficiency disrupts microglial inflammatory responses and membrane trafficking. Gene Expression Omnibus DataSets. https://www.ncbi.nlm.nih.gov/geo/query/acc.cgi?acc=GSE139592. Deposited 30 October 2019.